Title

New packer experiments and borehole logs in upper oceanic crust: Evidence for ridge-parallel consistency in crustal hydrogeological properties

Journal

Geochemistry Geophysics Geosystems, 14(8)

ISSN

1525-2027

Authors

Becker, Keir
Fisher, Andrew T
Tsuji, Takeshi

Publication Date

2013-08-01

DOI

10.1002/ggge.20201

Peer reviewed

Geochemistry Geophysics Geosystems G3

Article
Volume 14, Number 8
9 August 2013
doi: 10.1002/ggge.20201
ISSN: 1525-2027

Published by AGU and the Geochemical Society

New packer experiments and borehole logs in upper oceanic crust: Evidence for ridge-parallel consistency in crustal hydrogeological properties

Keir Becker
Division of Marine Geology and Geophysics, RSMAS, University of Miami, 4600 Rickenbacker Causeway, Miami, Florida 33149 USA (kbecker@rsmas.miami.edu)

Andrew T. Fisher
Earth and Planetary Sciences Department, University of California, Santa Cruz, California USA

Takeshi Tsuji
International Institute for Carbon-Neutral Energy Research (WPI-I2CNER), Kyushu University, Fukuoka, Japan

[1] We report new drillstring packer permeability tests conducted during Integrated Ocean Drilling Program (IODP) Expedition 327 in upper oceanic basement in Hole U1362A on the eastern flank of the Juan de Fuca Ridge. Hole U1362A lies within a closely spaced array (40–2460 m separation) of six holes in well-sedimented 3.5–3.6 m.y. old crust that were drilled, tested, and instrumented with borehole observatories during Ocean Drilling Program Leg 168 and IODP Expeditions 301 and 327. The permeability tests in Hole U1362A complement similar experiments previously conducted in nearby Holes 1026B, 1027C, and U1301B. The new results suggest consistency of upper crustal permeability between Holes U1362A and U1301B, which penetrate 290 and 320 m of basement and are separated by ~825 m. We obtain similar bulk permeability values of 1–3 $\times$ 10^{-12} m^2 for the sections deeper than ~150 m into basement in both holes. These values are significantly higher than results of packer experiments in the shallowest few tens of meters of basement in nearby Holes 1026B and 1027C, suggesting that the highest basement permeabilities in this area are not found in the shallowest basement layers. Downhole logs of density and penetration rate during drilling and coring in Holes U1362A and U1301B show similar trends within the upper crust, reinforcing the inference that there may be considerable lateral continuity in hydrogeologic properties. This continuity may be associated with the fundamental lithostratigraphy of the crust and/or influenced by ridge-parallel faulting and fracturing associated with the formation of abyssal hill topography.

Components: 8,671 words, 7 figures, 1 table.

Keywords: permeability; ocean crust.

Index Terms: 3021 Marine hydrogeology: Marine Geology and Geophysics; 3036 Ocean drilling: Marine Geology and Geophysics; 3017 Hydrothermal systems: Marine Geology and Geophysics; 0450 Hydrothermal systems: Biogeosciences; 1034 Hydrothermal systems: Geochemistry; 3616 Hydrothermal systems: Mineralogy and Petrology; 4832 Hydrothermal systems: Oceanography: Biological and Chemical; 8135 Hydrothermal systems: Tectonophysics; 8424 Hydrothermal systems: Volcanology; 5114 Permeability and porosity: Physical Properties of Rocks.

Received 29 January 2013; **Revised** 3 May 2013; **Accepted** 11 June 2013; **Published** 9 August 2013.

Becker K., A. T. Fisher, and T. Tsuji (2013), New packer experiments and borehole logs in upper oceanic crust: Evidence for ridge-parallel consistency in crustal hydrogeological properties, *Geochem. Geophys. Geosyst.*, *14*, 2900–2915, doi:10.1002/ggge.20201.

1. Introduction

[2] Since the late 1970s—shortly after the discovery of hydrothermal vents on the seafloor—scientific ocean drilling has provided important opportunities to constrain the permeability structure of the oceanic crust (as discussed in reviews by *Fisher* [1998], *Becker and Davis* [2004], *Fisher* [2005, and references therein]). Most drilling-based studies of ocean crustal hydrogeology have focused on young ridge flanks, areas far from the thermal, magmatic, and tectonic influence of active seafloor spreading. As in other fractured crystalline rock formations, the permeability of upper oceanic crust is likely to be highly heterogeneous, varying spatially by several orders of magnitude [e.g., *Khaleel*, 1989; *Gavrilenko and Gueguen*, 1998; *Neuman*, 2005]. In the upper oceanic crust, the hydrological connectivity that contributes to permeability at various spatial scales can be produced by a number of constructional and tectonic features, ranging from original eruptive stratigraphy to large-scale crustal faults. Permeability in such heterogeneous formations may be a scale-dependent tensor, governed by the direction(s) of both driving gradient and fluid flow, and with the distance and/or volume across which measurements are made [e.g., *Bear*, 1972; *Clauser*, 1992; *Rovey and Cherkauer*, 1995; *Zhou et al*., 2010]. Thus, the permeability of the upper ocean crust must be determined at multiple locations, spatial and temporal scales, and directions of interest, in order to fully resolve its influence on hydrogeologic and related (thermal, chemical, microbiological) processes.

[3] The methods that have been utilized since the 1970s in scientific ocean drilling to investigate ocean crustal permeability have included single-hole experiments that use either (1) drillstring packers to isolate sections of the formation for short-term pressure testing, pioneered by *Anderson and Zoback* [1982] or (2) observations of longer-term natural borehole flow into or out of the formation in holes left open to exchange with ocean bottom water [e.g., *Hyndman et al*., 1976; *Becker et al*., 1983, 2004; *Fisher et al*., 1997]. These indicate effective or bulk permeabilities of the tested formations at radial scales ranging from <1 m to hundreds of meters from the hole and thus may not represent conditions along full flow paths at the scale of hydrothermal flow through the ocean crust. Packer and free-flow experiments in single holes cannot be used to assess formation storage (compressive) properties, nor can they help in assessing azimuthal differences in permeability. Nevertheless, these measurements are valuable for assessing the stratigraphic distribution of permeable zones in the crust, based on measurements made by isolating different vertical intervals, and through comparison of values determined using the same techniques at multiple locations.

[4] Since the development of the sealed-hole "Circulation Obviation Retrofit Kit (CORK)" hydrogeological observatory in 1990 [*Davis et al*., 1992a], additional methods have become available to estimate crustal hydrologic properties at larger scales, in response to tectonic and tidal strains [e.g., *Davis et al*., 2000, 2001, 2004]. More recently, pressure changes in one borehole observatory were used to assess cross-hole formation response and properties resulting from perturbation at another observatory [*Fisher et al*., 2008; *Davis et al*., 2010].

[5] The earliest permeability tests in ocean crust at young ridge-flank sites suggested a three-layer structure to upper crustal permeability, with generally permeable upper few hundred meters of extrusives (pillows, flows, breccias) overlain by significantly less permeable sediments and underlain by significantly less permeable extrusives and intrusives [e.g., *Anderson et al*., 1985]. This overall structure is generally supported by more recent compilations at multiple ridge-flank sites [e.g., *Fisher*, 1998, 2005; *Becker and Davis*, 2004], although there are still very few results from deeper extrusives and intrusives. In addition, recent results with multiple methods suggest a scale dependence, with the methods that sense over greater scales usually producing larger values of average permeability [e.g., *Fisher*, 1998; *Becker and Davis*, 2003].

[6] Recent surveys have assessed the lateral distances across which ridge-flank hydrothermal circulation occurs. On 3.5–3.6 m.y. old seafloor on the eastern flank of the Juan de Fuca Ridge,

geochemical and thermal evidence indicates a travel path extending at least 50 km between volcanic edifices that are sites of recharge and discharge [*Fisher et al*., 2003a; *Hutnak et al*., 2006; *Wheat et al*., 2000]. Lateral fluid flow across tens of kilometers is also apparent on the eastern flank of the East Pacific Rise, near 10°N, where the seafloor is ~23 m.y. old [*Fisher et al*., 2003b; *Hutnak et al*., 2008; *Wheat and Fisher*, 2008]. To date, these are the only locations where ridge-flank hydrothermal recharge sites have been definitively located, and where the lateral scale of flow paths has been determined with confidence.

[7] In sum, borehole permeability tests suggest general consistency in the hydrogeologic layering of the upper ocean crust (with the greatest permeabilities found within thin zones of the upper extrusive layers), and other studies indicate sufficient lateral connectivity in flow paths so as to allow crustal-scale transport across vast distances (mining heat, discharging altered fluids, supplying nutrients to microbes, etc.). However, it remains unresolved whether such large-scale connectivity is produced by original igneous stratigraphy, discrete fault networks, and/or some combination of the two. Also, it remains to be shown whether permeable units in the crust are continuous at a scale of kilometers. It has been relatively rare in the history of scientific ocean drilling for multiple basement holes in the same area to be tested for hydrogeologic properties. Here we report the first subseafloor results that illustrate physical and hydrogeologic consistency of crustal properties at a kilometer scale, made possible when Expedition 327 of the Integrated Ocean Drilling Program (IODP) completed an array of holes in the Juan de Fuca Ridge flank.

2. Setting: The "Second Ridge" Array of ODP/IODP Boreholes

[8] IODP Expedition 327 revisited the "Second Ridge" area of 3.5 m.y. old crust on the sedimented eastern flank of the Juan de Fuca Ridge (Figure 1). Here Ocean Drilling Program (ODP) Leg 168 (1996) and IODP Expedition 301 (2004) had previously established four reentry holes that penetrated into oceanic basement beneath relatively thick cover of low-permeability sediments [*Davis et al*., 1997; *Fisher et al*., 2005a]. Earlier boreholes included Holes 1026B, U1301A, and U1301B along the axis-parallel, sediment-buried basement ridge, and 1027C in the thickly sedimented basement valley about 2 km to the east (Figure 1c). In each of these holes, packer tests were conducted to assess upper crustal hydrological properties [*Becker and Fisher*, 2000, 2008], and long-term CORK borehole observatories were installed [*Davis and Becker*, 2002; *Fisher et al*., 2005b]. The packer experiments in Hole U1301B indicate that the 170 m thick section of upper basement between 150 and 320 m subbasement (msb) is, on average, at least an order or magnitude more permeable than the shallowest few tens of meters of basement tested by the packer experiments in Holes 1026B and 1027C [*Becker and Fisher*, 2008].

[9] Expedition 327 returned to this area in 2010 [*Fisher et al*., 2011a, 2011b] and established two new reentry holes and CORK observatories in Holes U1362A and U1362B along the sediment-covered basement ridge between Holes 1026B and U1301B (Figure 1). Before installing the CORKs, geophysical and hydrologic properties were assessed with a logging program and packer experiments in Hole U1362A. The zone tested with the packer in Hole U1362A overlaps with the zones previously tested in Hole U1301B in terms of subseafloor and subbasement depths (Figure 2). This vertical overlap and the 825 m lateral separation between these sites provides for an initial assessment of the consistency of basement lithostratigraphy and permeability.

3. Hole U1362A Configuration and Experimental Methods

[10] Hole U1362A was drilled and cored to a total depth of 528 m below seafloor (mbsf), penetrating through 236 m of sediment and 292 m of volcanic basement rocks. Before any coring, the sediments and uppermost basement were drilled to 346 mbsf using a 0.37 m diameter bit and then cased to a depth of 308.5 mbsf (72.5 msb). Basement was then cored from 346 mbsf to total depth using a 0.25 m diameter bit. After cleanout operations were completed, rubble was tagged at 519 mbsf (283 msb); thus, there is at least 9 m of ambiguity as to the full depth extent of the open basement interval tested during subsequent packer measurements.

[11] Three passes of a single geophysical logging tool string were run in Hole U1362A to characterize upper basement properties and identify locations for placement of packers to be used for

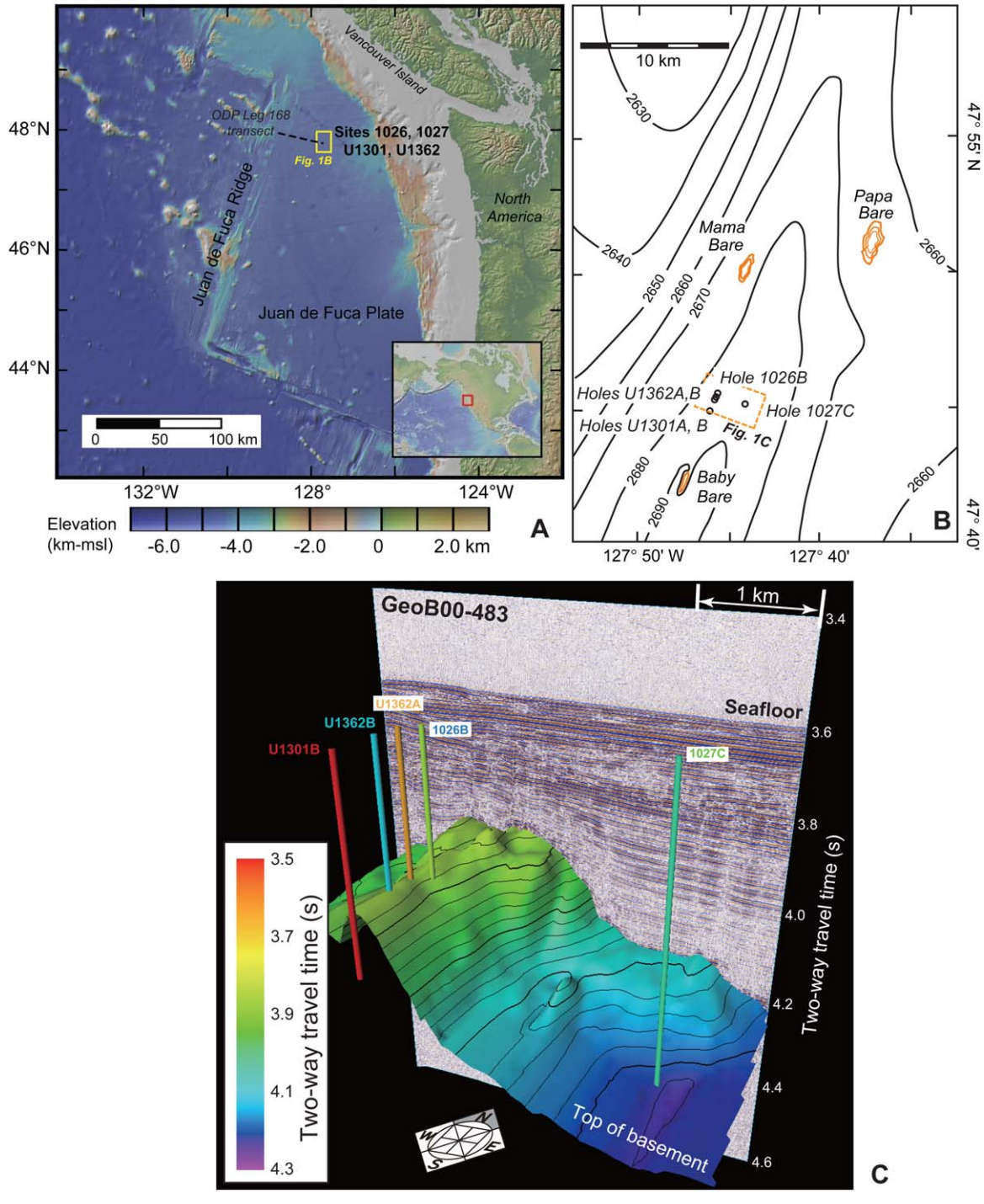

Figure 1. Location and general stratigraphy at borehole measurement locations (modified from *Fisher et al*. [2012]). (a) Map of the northeastern Pacific Ocean (location shown on inset), including major tectonic features and drill sites discussed in this paper. Dashed black line shows location of ODP Leg 168 drilling transect [*Davis et al*., 1997]. Yellow square shown in detail in Figure 1b. (b) Bathymetric contours (black, numbers in meters), basement outcrops (gold contours), and ODP and IODP drill holes (circles). Area in dashed yellow box is shown in Figure 1c. (c) Depth contours drawn on a surface showing the location of the sediment-basement interface in the Second Ridge drill area, and the locations of ODP and IODP drill holes. Surface plot is shown adjacent to a multichannel seismic reflection profile completed as part of a site survey prior to IODP Expedition 301 [*Zühlsdorff et al*., 2005]. The sediment-basement surface was created from numerous closely spaced seismic reflection profiles in the Second Ridge area. Depths are plotted in units of two-way travel time.

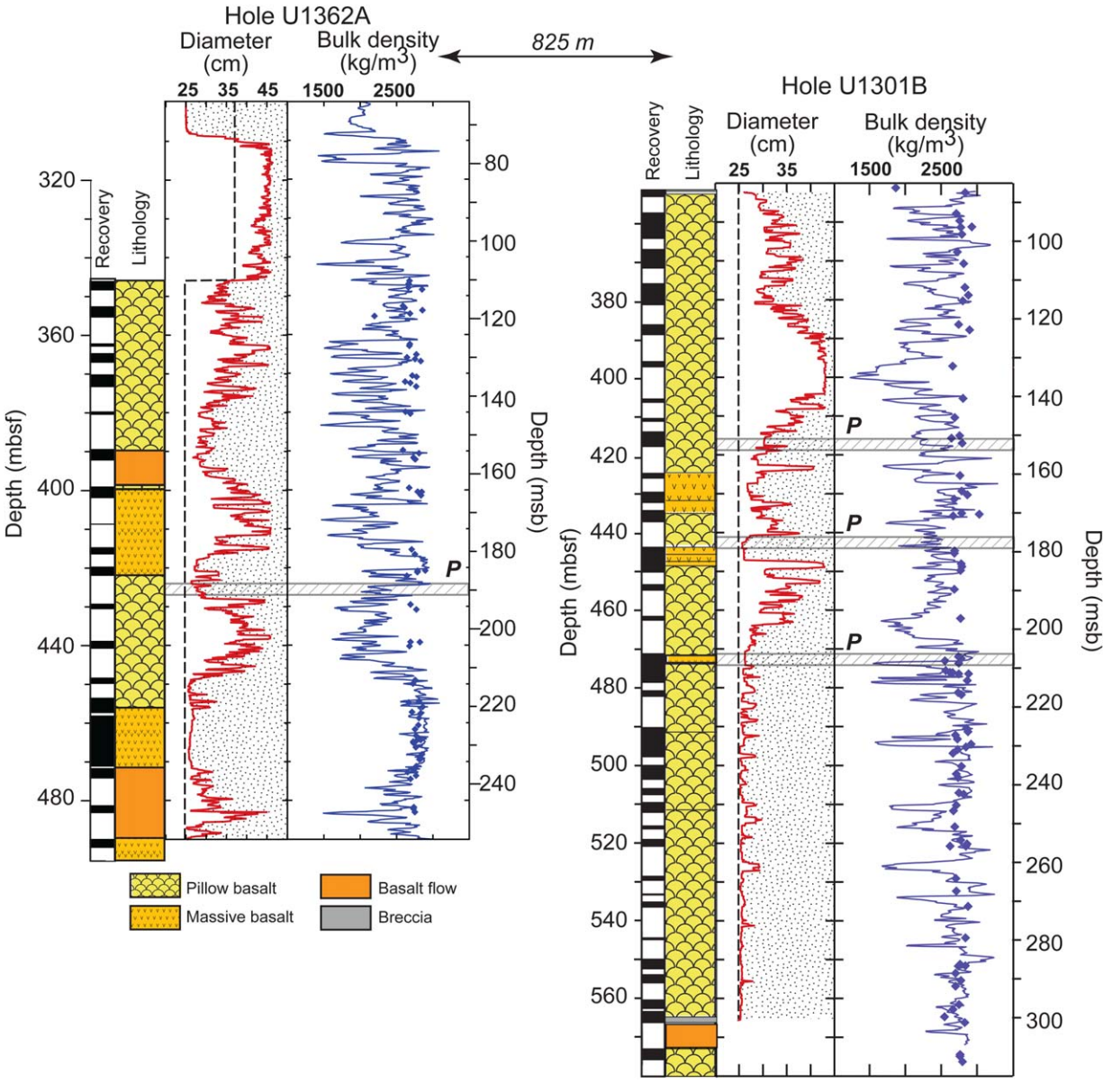

Figure 2. Borehole recovery, lithostratigraphy, diameter, and bulk density for Holes U1362A and U1301B (data from *Fisher et al*. [2005a, 2011]), which are separated laterally by ~825 m. Depths are shifted so that data in meters subbasement (msb) scale, right side of each borehole compilation, are aligned at the top of basement. Black/white bars indicate core recovery/nonrecovery, with recovered intervals pushed to top of cored intervals, based on IODP curatorial standards. Basement lithologies were identified mainly based on recovered core using different nomenclature during Expeditions 301 and 327 but have been standardized for this plot. Dashed lines in hole diameter columns indicate the size of drilling or coring bit used for corresponding interval, whereas red curve indicates diameter measured with mechanical caliper tool. Bulk density curve (blue) derived from geophysical logging data, whereas diamonds are laboratory measurements from hand samples. Horizontal bands labeled, "*P*," indicate position of inflatable packer elements used for permeability testing. Geophysical data begin near 100 mbsf, because shallower basement intervals were drilled and cased in each hole.

hydrogeologic testing and establishment of a CORK observatory. The main components of the tool string included a natural gamma ray detector, lithodensity tool, ultrasonic borehole imaging tool, and mechanical caliper [*Shipboard Scientific Party*, 2011]. The logging data were corrected to a common borehole depth reference using caliper and gamma ray logs to identify the deepest casing

shoe, below which the logging tools responded to the formation in open hole.

[12] Additional drilling information, including relative depth of the bit during drilling and coring operations, was collected at 2 s intervals using an updated version of the JOIDES *Resolution*'s rig-instrumentation system (RIS) [*Graber et al*., 2002]. RIS bit depths were determined for intervals of continuous downward movement of the drillstring, which extended up to 10 m during coring and up to 30 m during drilling (the lengths of a core barrel and a full stand of drill pipe, respectively). The most reliable depth and time information was used to calculate bit penetration rates and construct a profile of the variation of penetration rate versus depth in Hole U1362A.

[13] Hydrogeologic experiments during Leg 168 and Expeditions 301 and 327 were conducted using an inflatable packer assembled into the bottom of the drillstring, with methods as described by *Becker and Fisher* [2000, 2008] for previous experiments in Holes 1026B, 1027C, and U1301B. Once positioned at the intended sealing depth, the packer is activated after dropping down the drillstring a so-called "go-devil" that carries two electronic pressure gauges that monitor pressures just below the packer through the experiments. After it lands within the packer, the go-devil initially forces any seawater pumped from the rig floor into the inflation element until the packer expands and seals the hole After inflation, the go-devil then allows controlled pumping into the sealed formation zone beneath the inflated packer element. The packer can be inflated in casing to test the entire open-hole interval or in open hole if there are good indications (e.g., from downhole logs) of competent zones that will hold the inflated packer and allow it to seal off the section below.

[14] For typical ODP packer experiments in ridge-flank holes [e.g., *Becker and Fisher*, 2000, 2008], two types of pumping experiments are normally conducted. First are slug tests, in which the pumps are turned on briefly to apply a short pressure pulse to the isolated section; average permeability can be estimated from the decay of downhole pressures as the pressurized fluids flow into the formation. Second are constant-rate injection tests, particularly useful when permeability is high and slug test decay times are too rapid. These typically involve pumping into the formation at constant rate for time periods of 20 min to 2 h and then maintaining the seal of the pressurized hole for a similar time. Permeability can be estimated from the rise of downhole pressure during the period of injection, and in some cases from the decay of pressures after injection is stopped.

[15] Based on our prior experience in Holes 1026B and U1301B [*Becker and Fisher*, 2000, 2008], we expected slug tests to decay very rapidly and conducted only constant-rate injection tests in Hole U1362A. For constant-rate injection into a borehole that completely penetrates an isotropic, radially infinite, confined reservoir or aquifer, the expected pressure rise at any radial position in the reservoir relative to the injection hole is given by the classic *Theis* [1935] solution. This involves an exponential integral to represent the injection hole as a vertical line source; the pressure response at a given position depends on time, injection rate, and reservoir transmissivity. Transmissivity is defined as the product of reservoir thickness and hydraulic conductivity K, which is related to permeability (k) by $k = K\mu/\rho g$, with μ and ρg being the viscosity and specific weight of the fluid, respectively.

[16] Results presented in this paper were derived by fitting observed pressure responses during injection to this idealized solution, using a nonlinear least squares approach to minimize misfit. When the pressure observations are made in the injection hole, radial symmetry of aquifer properties must be assumed, but the solution can be modified to account for the source hole penetrating only part of the permeable aquifer. As part of the analysis, we explored a range of thicknesses of the open borehole interval, thicknesses of the upper crustal aquifer, and alternative borehole/formation models. We examined results using more complex models of crustal properties but found no statistical fit improvement relative to the *Theis* [1935] solution.

4. Experimental Results

[17] Borehole geophysical logs from uppermost basement in Hole U1362A are similar to those collected in Hole U1301B and the upper few hundred meters of other oceanic boreholes drilled into the extrusive section of young ocean crust [e.g., *Bartetzko and Fisher*, 2008; *Matthews et al*., 1984; *Pezard and Anderson*, 1989]. The crust around Hole U1362A is highly layered, at a vertical scale of 5–40 m, and the hole is enlarged beyond bit size (and sometimes beyond caliper size) across numerous depth intervals (Figure 2). There is generally a good inverse correlation between the caliper and bulk density logs, with larger-diameter

intervals tending to have lower bulk density. This correlation may be real, because less dense intervals tend to be weaker and thus wash out more easily during drilling and coring, or it may result from imperfect contact between the borehole wall and the logging sonde in washed out and irregular intervals.

[18] Intervals with hole diameters close to bit size and higher bulk densities, across depth intervals of 10–20 m or more, were good candidates for packer seats (Figure 2). The seat selected in Hole U1362A for hydrogeologic testing was near 426.5 mbsf (190.5 msb), separating two borehole zones ~20 m thick that are severely washed out ("over gauge" according to the caliper log). After conducting successful packer tests at this inflation depth, we deflated the element and repositioned the packer in casing for an inflation intended to test the entire open-hole basement interval, but that attempt failed because of damage to the inflation element incurred on moving the packer in the hole.

[19] The downhole pressure record from the successful inflation (Figure 3a) shows the overall sequence of (*H*) a hydrostatic reference at 424.5 mbsf before packer inflation, the actual inflation (*I*) after repositioning the packer two m deeper, a sealed-hole borehole reference (*B*) that is below the hydrostatic reference because of the residual effects of a downhole flow of cold ocean bottom water induced by drilling operations, the pressure increases during 2 h long periods of constant-rate injection into the isolated zone at 4.4 and 8.4 L/s, and then packer deflation (*D*) and a second hydrostatic reference period (*H*2). In 2004, there was a large tidal variation in seafloor pressure during the time when packer experiments were conducted in Hole U1301B, and this required careful correction of the downhole pressures [*Becker and Fisher*, 2008]. In contrast, there was a smaller tidal range in this area (measured at nearby Hole 1027C) at the time of the Expedition 327 packer tests in Hole U1362A (Figure 3b), so no significant tidal correction was required.

[20] Figures 4a and 4b show downhole pressure records for two hour-long injection tests conducted in Hole U1362A at constant pumping rates of 4.4 and 8.4 L/s, respectively. Given that the near-hole region had been severely cooled by drilling-induced downhole flow of cold ocean bottom water, we used a seawater viscosity of 1.6×10^{-3} Pa s, appropriate for a temperature of ~2°C, as indicated by the downhole gauges (Figure 3a). In addition to the expected rise of pressure during injection, there are two other features to the pressure response that are important to note. First are the almost immediate pressure drops when injection was stopped and the hole was kept "shut-in" without venting downhole pressure; this quick recovery response requires high formation permeability. Second, there are slight offsets in the baseline pressure values before and after injection, particularly for the first test (dotted lines). Applying a baseline correction to account for these trends makes little difference for the interpreted permeability.

[21] Figures 4c and 4d show fits to the data to the Theis model, and Table 1 summarizes test results, including a range of possible aquifer thicknesses. Varying the aquifer thickness results in proportionally different transmissivity values but little difference in calculated bulk permeability. Correcting the data for the small offset in pressure baseline for the first injection test results in a slightly greater permeability, but overall the results are all consistent with a bulk permeability of $1.2–1.7 \times 10^{-12}$ m^2 for the first injection test, and $0.9–1.1 \times 10^{-12}$ m^2 for the second injection test at higher rate.

5. Discussion

5.1. Comparison to Results From Nearby Holes

[22] The apparent permeability values obtained for the tested zone in Hole U1362A for two injection tests are very similar to the values of $1–3 \times 10^{-12}$ m^2 reported by *Becker and Fisher* [2008] for seven injection tests in three comparable test intervals (152–318 m into basement) in Hole U1301B, located 825 m NNE of Hole U1362A (Figure 5). The values deeper than ~150 msb in both holes are higher by roughly an order of magnitude than the values obtained by *Becker and Fisher* [2000] in the shallowest basement sections in nearby Holes 1026B and 1027C. This suggests that the highest upper crustal permeabilities in this region are not found immediately adjacent to the sediment-basement interface but are deeper in the extrusive section [*Fisher et al.*, 2008; *Becker and Fisher*, 2008]. Holes 1026B and 1027C each penetrated <50 m into uppermost basement, sampling only a few igneous units with relatively poor core recovery and no supporting logging data. Possible explanations for lower permeability in these uppermost

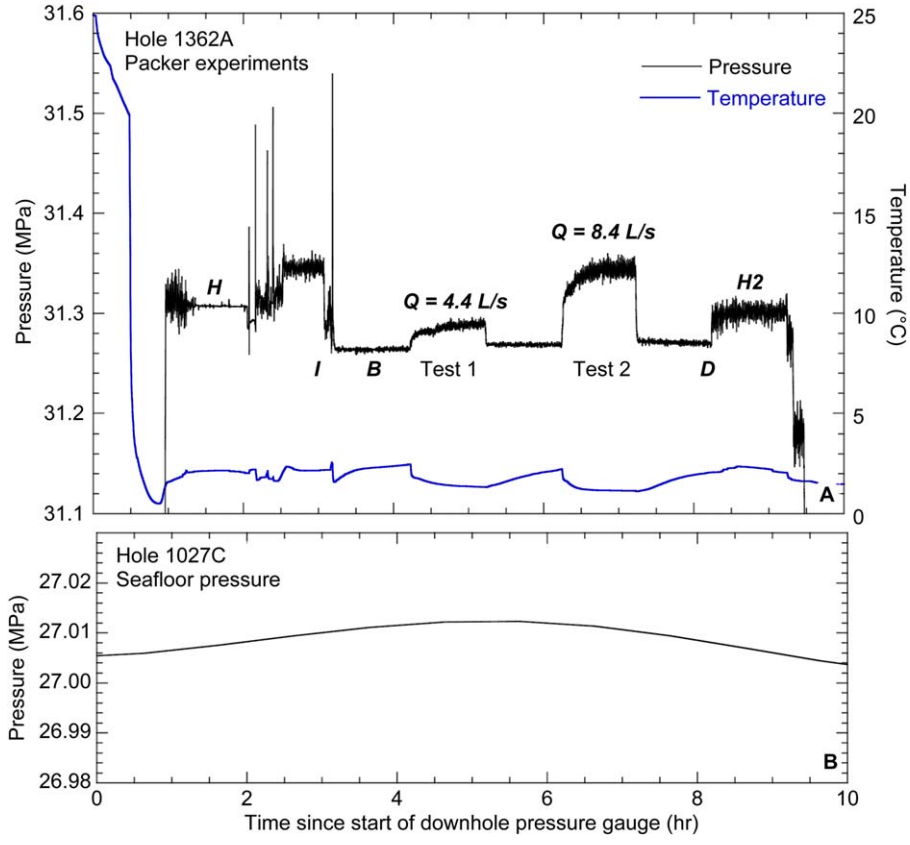

Figure 3. Downhole pressure and temperature data from Hole U1362A during packer testing and seafloor pressure data from nearby Hole 1027C. (a) Downhole pressure and temperature data during packer experiments in Hole U1362A on IODP Expedition 327. Pressure data (solid line) show gauge descent in go-devil, hydrostatic readings (*H*) with gauge held in packer prior to inflation, packer inflation (*I*), zone baseline pressure (*B*), pressures during tests with two flow rates ($Q = 4.4$ and 8.4 L/s), packer element deflation (*D*), and gauge recovery. Note relatively low temperatures from throughout period of packer testing, as a result of pumping cold water down borehole during drilling, coring, casing, and other operations. Temperatures drop when pumps are on, then rise slightly during periods when pumping is suspended. (b) Seafloor pressures at Hole 1027C, located ~2300 m east of Hole U1362A (Figure 1), recovered during CORK servicing with the ROV Jason, in summer 2011 [*Fisher et al*., 2012]. The small variations in seafloor pressure at Hole 1027C result mainly from oceanic tides, which were modest during the time of packer testing in Hole U1362A (total variation during individual tests is ≤5 kPa, equivalent to ≤0.5 m of water depth).

sections, relative to deeper intervals, could include lower probability of sampling any significant fractures or faults, reduced lateral continuity of the youngest basement units because of waning magma supply or roughness along the basement-sediment contact, or clogging due to more intense alteration.

[23] *Becker and Fisher* [2008] tested the borehole permeability of three overlapping zones in Hole 1301B (Figures 2, 5, and 6). A comparison of caliper and geophysical logs from Holes U1301B and U1362A guided selection of the packer seat in Hole U1362A and suggests that there may be a hydrostratigraphic correlation between the two holes. In particular, similar patterns in the caliper and penetration rate records (Figure 6) suggest that the packer seat in Hole U1362A corresponds most closely to the middle packer seat in Hole U1301B.

[24] An additional penetration rate record was generated for Hole U1362B, located between Holes U1301B and U1362A (Figures 1 and 6), and drilled into basement and cased without coring or geophysical measurements. Penetration rate records derived from RIS data need to be interpreted cautiously because there are many factors other than lithologic properties that can influence this parameter, including bit diameter and type, weight on bit, the extent of hole cleaning, and fluid circulation rate. In the absence of core and geophysical data from Hole U1362B, there is no way

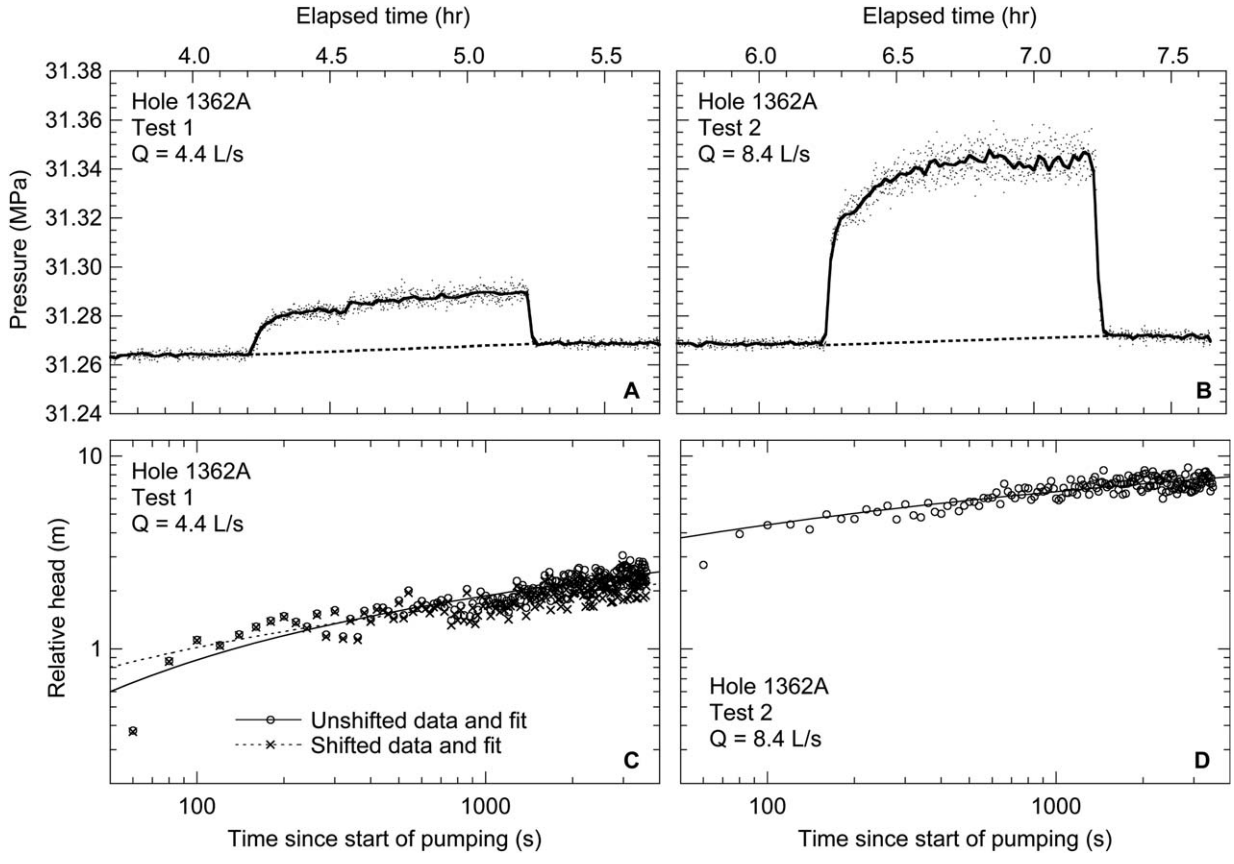

Figure 4. Detail plots and fits from individual packer flow tests in Hole U1362A. (a) Detail plot of first packer flow test, with $Q = 4.4$ L/s. Dots show individual pressure readings, collected every 5 s, and solid line shows pressure data smoothed with a 72 s boxcar filter. Dashed line shows linear trend between pressure baseline at start and end of test. (b) Detail plot of first packer flow test, with $Q = 4.4$ L/s, with symbols as in Figure 4a. (c) Plot of pressure observations (converted to equivalent head, log scale) during first packer flow test in Hole U1362A. Open circles show raw data, whereas cross symbols show data after applying a linear baseline shift. Solid and dashed lines show least squares best fit of the *Theis* [1935] model to data, neglecting first 100 s of pumping time period. (d) Plot of pressure observations (converted to equivalent head, log scale) during second packer flow test in Hole U1362A. Solid line shows fit of *Theis* [1935] model, neglecting first 100 s of data.

to test whether lateral consistency apparent in the penetration rate records is indicative of primary lithology or formation structure. That said, there appear to be consistent patterns in higher and lower penetration rates measured across the three holes, suggesting some continuity in formation properties along a distance of ~825 m (Figure 6).

[25] The similarity in upper basement permeability values in Holes U1301B and U1362A, when combined with the consistency in downhole patterns in geophysical log responses and penetration rates, suggests that there may be lateral continuity in formation petrophysical and hydrogeologic properties in this area. This continuity would apply along a direction indicated by the hole-to-hole orientation, N20°E (Hole U1362A to Hole U1301B), roughly parallel to the active spreading center located 100 km to the west (Figure 1).

[26] In Hole U1301B, packer tests from the deepest setting depth (~207 msb) indicated that the 111 m of open hole below that depth was significantly less permeable than the overlying basement section. This would support an interpretation in Hole U1362A based on using the drilled thickness to represent the "reservoir" thickness; either the permeable section does not extend to significantly greater depth, or crustal layering restricts vertical transport more than horizontal transport. Packer results from Hole U1301B also suggest that the ~20 m thick larger-diameter zone at ~445–465 mbsf (~180–200 msb) may have a permeability as great as 2×10^{-11} m^2. A similar ~20 m thick

Table 1. Summary of Results of Applying *Theis* [1935] Model to Packer Injection Tests in Hole U1362A[a]

Test ID and Rate (L/s)	Baseline Correction Applied?	Aquifer Thickness (m)	K_z/K_r[b]	Transmissivity (10^{-3} m^2/s)	Hydraulic Conductivity (10^{-6} m/s)	Permeability (10^{-12} m^3)
#1, 4.35	No	100	1	0.77	7.65	1.20
	No	290	1	2.21	7.61	1.19
	No	600	1	0.45	7.56	1.19
	No	290	0.01	2.22	7.64	1.20
	Yes	290	1	3.16	10.9	1.71
#2, 8.36	No	290	1	2.02	6.97	1.09

[a]All processing used the following parameters: fluid temperature 2°C, fluid viscosity 1.60×10^{-3} Pa s, fluid density 1040 kg/m^3, gravitational acceleration 9.81 m^2/s, first 100 s of data ignored in curve fit.
[b]K_z/K_r is ratio of vertical to horizontal hydraulic conductivity.

large-diameter zone was sampled directly below the packer seat in Hole U1362A (Figures 2 and 6). If most of the transmissivity in the tested interval in Hole U1362A is assigned to this large-diameter zone, as suggested by results in Hole U1301B, then the permeability of that zone also may be as high as $\sim 10^{-11}$ m^2 (Figure 5).

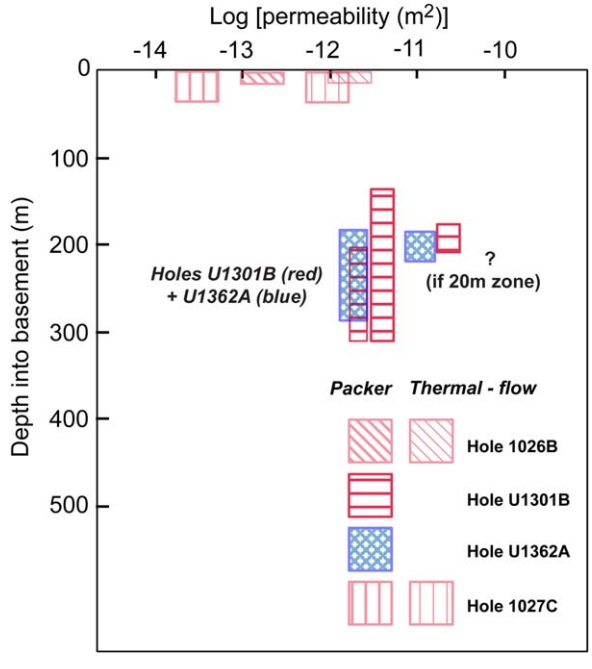

Figure 5. Comparison of bulk permeability values in Hole U1362A with previous results from Holes 1026B, 1027C, and U1301B located on 3.5–3.6 m.y. old seafloor in the same area [*Becker and Fisher*, 2000, 2008]. Each measurement is represented by a rectangle with vertical extent that corresponds to the zone isolated by the packer and horizontal extent that represents interpreted uncertainty in the bulk permeability. The question mark corresponds to interpretations in Holes U1301B and U1362A based on assigning majority of transmissivity to ~20 m thick large-diameter zones directly beneath the packer seat in Hole U1362A and between the intermediate and deep packer seats in Hole U1301B (Figure 2).

5.2. Relation to Regional Surveys and Core Samples From Boreholes

[27] The inferred continuity of geophysical and hydrogeologic properties around Holes U1301B and U1362A is consistent with results of numerous geophysical and geological studies that sample the upper ocean crust at a range of spatial averaging scales. Reflection seismic surveys have commonly suggested the presence of a layered velocity structure in the upper crust along and near the Juan de Fuca Ridge, with lateral continuity on a scale of kilometers [e.g., *Canales et al*., 2005; *Carbotte et al*., 2008; *Nedimovic et al*., 2008; *Christeson et al*., 2010]. Seafloor geological and mapping studies of medium-rate spreading centers have similarly found that individual eruptive and lithologic units may extend laterally on the order of one to several kilometers [e.g., *Chadwick and Embley*, 1994; *Chadwick et al*., 1998, 2001; *Colman et al*., 2012; *Kappel and Ryan*, 1986]. Additional evidence for the continuity of individual upper crustal layers at a kilometer scale comes from studies of tectonically exposed cross sections and ophiolites [e.g., *Karson*, 2002; *Karson et al*., 2002; *Schmincke and Bednarz*, 1990], and modeling of submarine eruptive processes [e.g., *Gregg and Fornari*, 1998; *Zhu et al*., 2003].

[28] In contrast, cores recovered from Holes U1301B and U1362A are challenging to correlate on the basis of petrology and alteration as observed in hand samples. On the southern flank of the Costa Rica Rift, a similar lack of unit-by-unit correlation was noted by *Alt et al*. [1996], based on examination of cores recovered from Holes 504B and 896A ~1 km apart (although the separation of these holes is in a ridge-perpendicular sense, whereas the separation in the present study is ridge-parallel). The lack of obvious unit-by-unit correlation between boreholes based on hand samples is not surprising, as

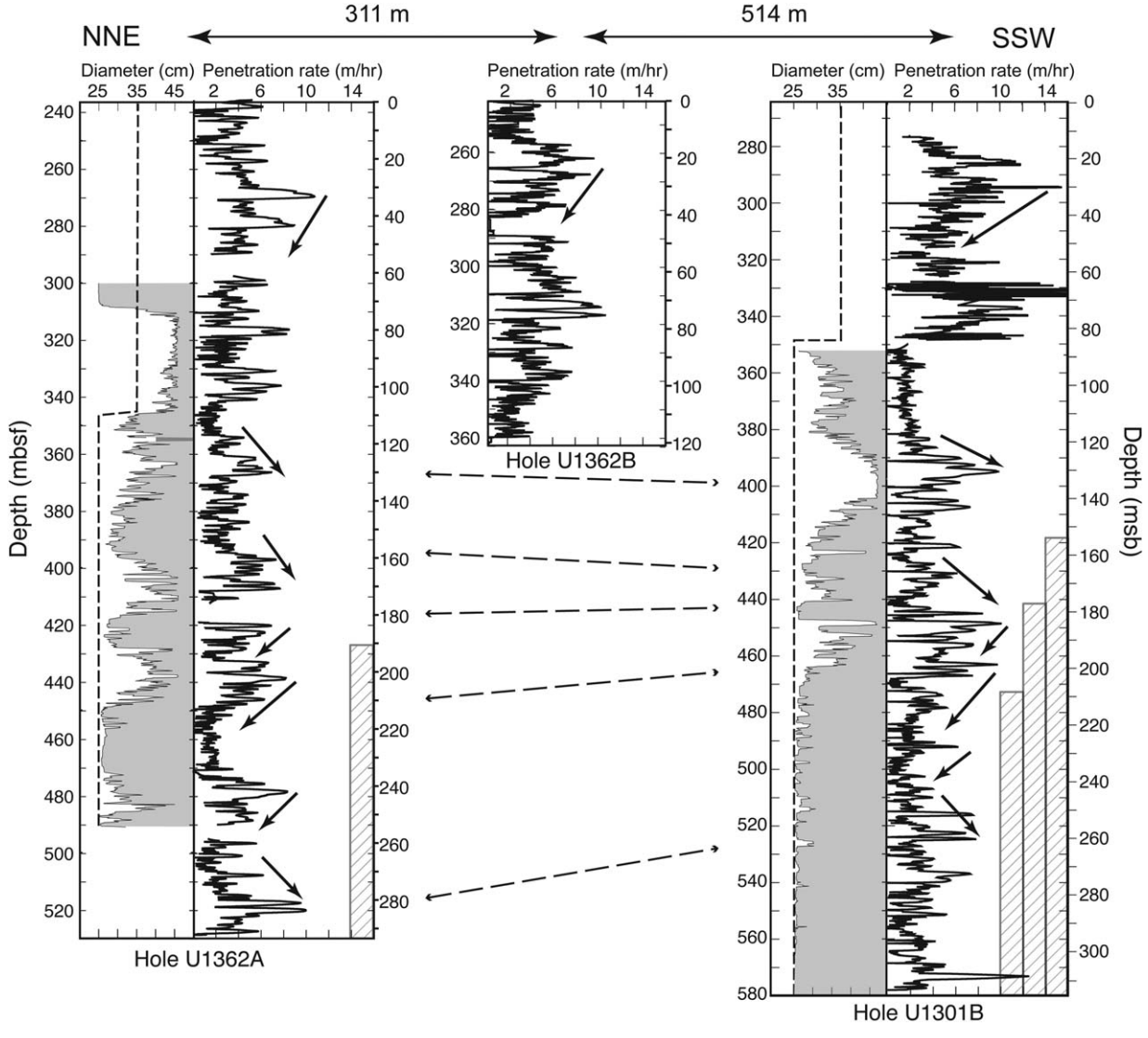

Figure 6. Hole diameters and drilling/coring penetration rates for Holes U1362A, U1362B, and U1301B. Diameter data for Holes U1362A and U1301B are as shown in Figure 2, with dashed lines indicating bit size. No diameter data are available for Hole U1362B, because there was no geophysical logging program in this hole. Apparent penetration rates during drilling and coring were derived from the first pass of the drill bit, recorded every 2 s with the rig-instrumentation system, as described in the text. Solid arrows drawn adjacent to parts of the penetration rate data indicate short-interval trends that appear to be correlatable between holes. On the basis of these qualitative trends, and on the general shape of the borehole diameter data, we have proposed lateral correlations between sections of the downhole records, as indicated with dashed arrows. Although these correlations are imperfect, they are consistent with the similarity of packer test results in Holes U1362A and U1301B, and with evidence for lateral continuity in extrusive units mapped at spreading centers and tectonic exposures of the ocean crust, and in ophiolites.

there are common small-scale variations in the frequency and form of eruptive units and the extent of fracturing and rock alteration in the upper crust. In addition, core recovery from boreholes in the upper ocean crust is generally low and likely to be biased against representation by less robust intervals (which may be among the most permeable and thus most represented in borehole testing).

[29] As noted by *Pezard et al*. [1992] in articulating a model for accretion of intermediate-rate crust, the flow units of largest lateral extent may constitute vertical permeability barriers within an upper crustal layer of generally high horizontal permeability. Thus, the apparent lateral consistency we report may not be linked to continuity of individual eruptive units. Instead, it may indicate

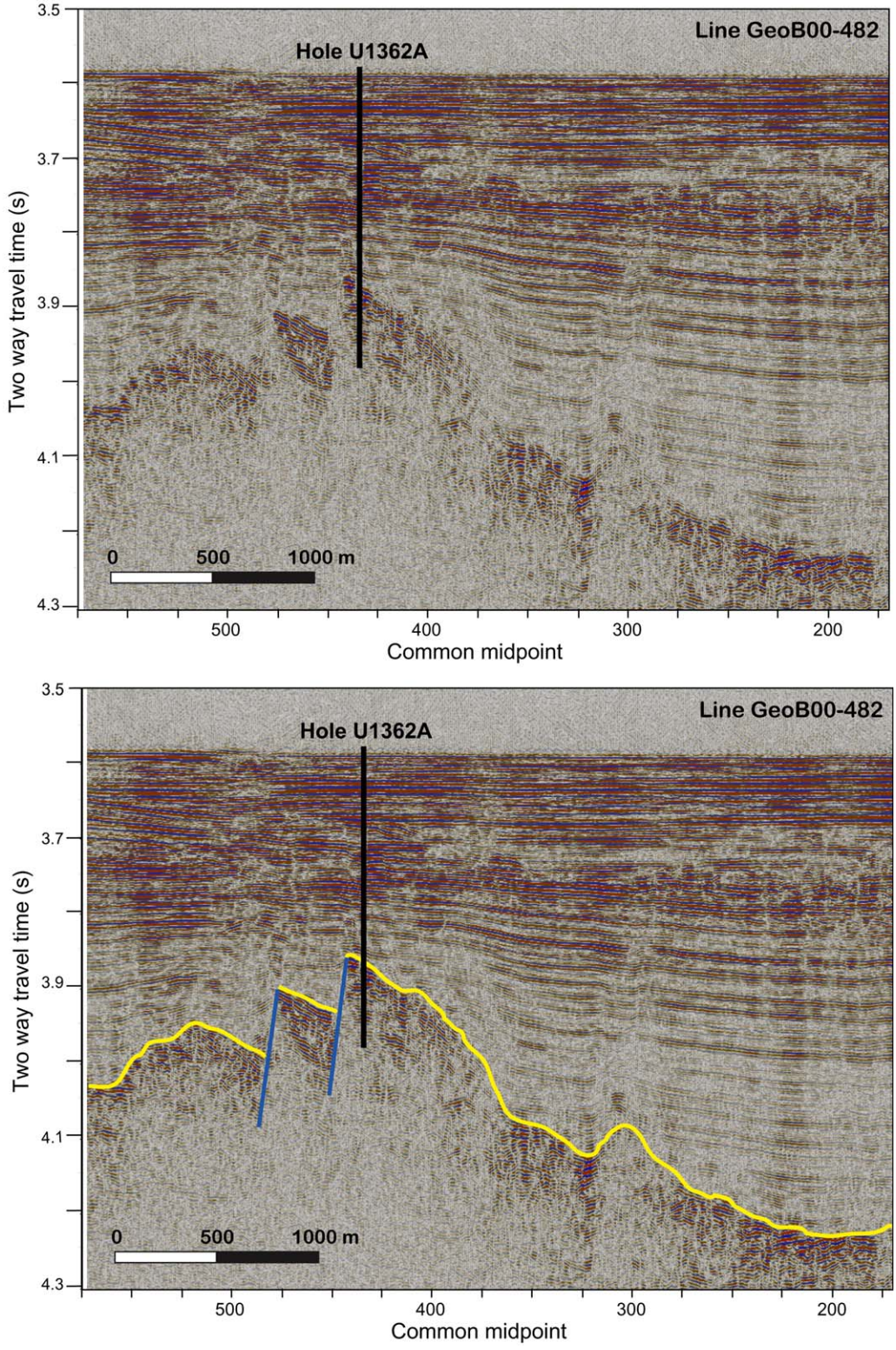

Figure 7. Seismic reflection line GeoB00–482 of *Zühlsdorff et al*. [2005] that crosses the location of Hole U1362A, at an orientation that is normal to the strike of the Second Ridge sediment covered basement ridge shown in Figure 1. (top) A redisplay of the processed data shown in Figure F8C of *Zühlsdorff et al*. [2005]. (bottom) The sediment-basement contact (yellow) and high-angle normal faults (blue) that are subparallel to the strike of the basement ridge and may contribute to along-strike continuity of hydrogeological properties.

the generally high permeability of the upper volcanic layer composed of multiple eruptive units, which are confined by more massive flow units having lower vertical permeability.

[30] Alternatively or in addition, the apparent consistency of formation stratigraphy and hydrogeologic properties between Holes U1362A and U1301B could represent a component of tectonic modification associated with ridge-flank faulting. These holes are located near the top of a single basement high, the peak of an abyssal hill formed by stretching of the brittle upper crust [e.g., *Kappel and Ryan*, 1986; *Macdonald et al*., 1996; *Buck and Poliakov*, 1998]. Careful examination of seismic reflection profiles running perpendicular to this basement high (e.g., Figure 7) shows that these boreholes are located close to high-angle normal faults that are oriented subparallel to the active spreading center to the west [*Davis et al*., 1992b; *Zühlsdorff et al*., 2005; *Hutnak et al*., 2006]. The same stresses that generated these faults could have imparted smaller-scale fractures that influence the hydrogeologic fabric of the crust more generally. Azimuthal anisotropy in upper crustal permeability, with the long axis of the permeability ellipse oriented in the ridge-parallel direction (N20°E), could help to explain the difference in properties inferred from cross-hole response and those inferred from single-hole tests [*Fisher et al*., 2008]. High-angle faulting is also thought to have influenced crustal hydrogeology around Hole 504B [*Ayadi et al*., 1998], although there is less information available in that area concerning spatial continuity of upper crustal layers or the layered distribution of permeability.

6. Conclusions

[31] Results of packer tests and borehole logs run in Hole U1362A during IODP Expedition 327 suggest significant consistency in formation properties when compared to data sets from nearby Hole U1301B. These two holes penetrate 290 and 320 m, respectively, into the basaltic upper crust and are separated by ~825 m along a sediment-covered basement ridge that strikes parallel to the spreading center to the west. The packer experiments in both holes indicate bulk permeability values of $1–3 \times 10^{-12}$ m^2 for the open-hole sections deeper beneath 236–265 m of much less permeable sediment. The permeability of basement sections tested in Holes U1301B and U1362A is significantly greater than indicated by packer experiments in the shallowest few tens of meters of basement in nearby Holes 1026B and 1027C, suggesting that the largest basement permeabilities in this area are not found immediately adjacent to the sediment-basement interface. Downhole logs of density and penetration rate in Holes U1362A and U1301B show similar trends within the permeable sections, suggesting that there may be some lateral continuity associated with these zones. This consistency, and the lack of obvious lithologic (petrologic, alteration) correlation based on hand samples from cores, suggests that hydrogeologic continuity could be defined by generally permeable volcanic units bounded by more massive flows, and/or the extent of ridge-parallel crustal fabric associated with abyssal hill topography.

[32] Additional insights as to the lateral extent of hydrogeologic connection within the ocean crust in this area will come from ongoing hydrogeologic studies using the borehole observatory network at Sites 1026, 1027, U1301, and U1362. Tracers injected into the upper crust around Hole U1362B during Expedition 327 [*Fisher et al*., 2011c] are currently being sampled by autonomous collection systems in surrounding holes and will provide the most direct evidence of both lateral connection in the crust and rates of transport. The pressure response to fluid and tracer injection during Expedition 327, and to a multiyear free-flow experiment, will allow a more accurate and nuanced assessment of both large-scale hydrogeologic properties and azimuthal anisotropy in the upper crust [*Fisher et al*., 2011c, 2012]. Mapping the nature of the permeable network that guides fluid, heat, solute, and microbial transport in the ocean crust is challenging, but considerable progress can be made by combining multidisciplinary data collected across a range of spatial and temporal scales.

Acknowledgments

[33] We thank the technicians, officers, and crew of the J. Resolution for assistance in running packer experiments during IODP Expedition 301. This paper was improved significantly after perceptive reviews by R. Carlson, Associate Editor W. Wilcock, and an anonymous reviewer. This research used additional data provided by the IODP and was supported by NSF grant OCE-1030350 and Consortium for Ocean Leadership (COL) project T327B8 (K.B.), NSF grants OCE-0939564 and 1031808 (A.T. F.), and COL projects T327A7 and T327B7 (A.T.F.). This is C-DEBI contribution 163.

References

Alt, J. C., D. A. H. Teagle, C. Laverne, D. A. Vanko, W. Bach, J. Honnorez, K. Becker, M. Ayadi, and P. A. Pezard (1996), Ridge-flank alteration of upper ocean crust in the eastern Pacific: Synthesis of results for volcanic rocks of Holes 504B and 896A, *Proc. Ocean Drill. Program Sci. Results*, *148*, 435–450.

Anderson, R. N., and M. D. Zoback (1982), Permeability, underpressures and convection in the oceanic crust near the Costa Rica Rift, eastern equatorial Pacific, *J. Geophys. Res.*, *87*(B4), 2860–2868, doi:10.1029/JB087iB04p02860.

Anderson, R. N., M. D. Zoback, S. H. Hickman, and R. L. Newmark (1985), Permeability versus depth in the upper oceanic crust: In-situ measurements in DSDP Hole 504B, eastern equatorial Pacific, *J. Geophys. Res.*, *90*(B5), 3659–3669, doi:10.1029/JB090iB05p03659.

Ayadi, M., P. A. Pezard, G. Bronner, P. Tartarotti, and C. Laverne (1998), *Multi-scalar structure at the DSDP/ODP Site 504, Costa Rica Rift: III. Faulting and fluid circulation constraints from integration of FMS images, downhole logs, and core data, in Core-Log Integration*, edited by P. K. Harvey and M. A. Lovells, Geol. Soc. London Spec. Publ., *136*, 311–326.

Bartetzko, A., and A. T. Fisher (2008), Physical properties of young (3.5 m.y.) oceanic crust from the eastern flank of Juan de Fuca Ridge: Comparison of wireline and core measurements with global data, *J. Geophys. Res.*, *113*, B05105, doi:10.1029/2007JB005268.

Bear, J. (1972), *Dynamics of Fluids in Porous Media*, Elsevier, New York.

Becker, K., and E. E. Davis (2003), New evidence for age variation and scale effects of permeabilities of young oceanic crust from borehole thermal and pressure measurements, *Earth Planet. Sci. Lett.*, *210*, 499–508.

Becker, K. and E. E. Davis (2004), *In situ determinations of the permeability of the igneous oceanic crust, in Hydrogeology of the Oceanic Lithosphere*, edited by E. E. Davis and H. Elderfield, pp. 189–224, Cambridge Univ. Press, Cambridge.

Becker, K. and A. T. Fisher (2000), Permeability of upper oceanic basement on the eastern flank of the Endeavor Ridge determined with drill-string packer experiments, *J. Geophys. Res.*, *105*(B1), 897–912.

Becker, K. and A. T. Fisher (2008), Borehole packer test at multiple depths resolve distinct hydrologic intervals in 3.5-Ma oceanic crust on the eastern flank of Juan de Fuca Ridge, *J. Geophys. Res.*, *113*, B07105, doi:10.1029/2007JB005446.

Becker, K., M. G. Langseth, R. P. Von Herzen, and R. N. Anderson (1983), Deep crustal geothermal measurements, Hole 504B, Costa Rica Rift, *J. Geophys. Res.*, *88*(B4), 3447–3457, doi:10.1029/JB088iB04p03447.

Becker, K., E. E. Davis, F. N. Spiess, and C. P. deMoustier (2004), Temperature and video logs from the upper oceanic crust, Holes 504B and 896A, Costa Rica Rift flank: Implications for the permeability of upper oceanic crust, *Earth Planet. Sci. Lett.*, *222*, 881–896.

Buck, W. R., and A. N. B. Poliakov (1998), Abyssal hills formed by stretching oceanic lithosphere, *Nature*, *392*, 272–275.

Canales, J. P., R. S. Detrick, S. M. Carbotte, G. M. Kent, J. B. Diebold, A. Harding, J. Babcock, M. Nedimovic, and E. Van Ark (2005), Upper crustal structure and axial topography at intermediate-spreading ridges: Seismic constraints from the southern Juan de Fuca Ridge, *J. Geophys. Res.*, *110*, B12104, doi:10.1029/2005JB003630.

Carbotte, S. M., M. Nedimovic, J. P. Canales, G. M. Kent, A. J. Harding, and M. Marjanovic (2008), Variable crustal structure along the Juan de Fuca Ridge: Influence of on-axis hotspots and absolute plate motions, *Geochem. Geophys. Geosyst.*, *9*, Q08001, doi:10.1029/2007GC001922.

Chadwick, W. W., Jr., and R. W. Embley (1994), Lava flows from a mid-1980s submarine eruption on the Cleft Segment, Juan de Fuca Ridge, *J. Geophys. Res.*, *99*(B3), 4761–4776, doi:10.1029/93JB02041.

Chadwick, W. W., Jr., R. W. Embley, and T. M. Shank (1998), The 1996 Gorda Ridge eruption: Geologic mapping, sidescan sonor, and SeaBeam comparison results, *Deep Sea Res*. II, *45*, 2547–2569.

Chadwick, W. W., Jr., D. S. Scheirer, R. W. Embley, and H. P. Johnson (2001), High-resolution bathymetric surveys using scanning sonars: Lava morphology, hydrothermal vents, and geologic structure at recent eruption sites on the Juan de Fuca Ridge, *J. Geophys. Res.*, *106*(B8), 16,075–16,099, doi:10.1029/2001JB000297.

Christeson, G. L., J. A. Karson, and K. D. McIntosh (2010), Mapping of seismic layer 2A/2B boundary above the sheeted duke unit at intermediate spreading crust exposed near the Blanco Transform, *Geochem. Geophys. Geosyst.*, *11*, Q03015, doi:10.1029/2009GC002864.

Clauser, C. (1992), Permeability of crystalline rocks, *Eos Trans. AGU*, *73*, 233, 237–238.

Colman, A., et al. (2012), Effects of variable magma supply on mid-ocean ridge eruptions: Constraints from mapped lava flow fields along the Galapagos Spreading Center, *Geochem. Geophys. Geosyst.*, *13*, Q08014, doi:08010.01029/02012GC004163.

Davis, E. E., and K. Becker (2002), Observations of natural-state fluid pressures and temperatures in young oceanic crust and inferences regarding hydrothermal circulation, *Earth Planet. Sci Lett.*, *204*, 231–248.

Davis, E., K. Becker, T. Pettigrew, B. Carson, and R. Macdonald (1992a), CORK: A hydrologic seal and downhole observatory for deep ocean boreholes, *Proc. Ocean Drill. Program Initial Rep.*, *139*, 43–53.

Davis, E. E., et al. (1992b), FlankFlux: An experiment to study the nature of hydrothermal circulation in young oceanic crust, *Can. J. Earth Sci.*, *29*(5), 925–952.

Davis, E. E., M. J. Mottl, A. T. Fisher, and J. Firth (1997), *Proceedings of the Ocean Drilling Program, Initial Reports*, vol. *168*, 470 pp., Ocean Drill. Program, College Station, Tex.

Davis, E. E., K. Wang, K. Becker, and R. Thomson (2000), Formation-scale hydraulic and mechanical properties of oceanic crust inferred from pore-pressure response to periodic seafloor loading, *J. Geophys. Res.*, *105*(B6), 13,423–13,435, doi:10.1029/2000JB900084.

Davis, E. E., K. Wang, R. E. Thomson, K. Becker, and J. F. Cassidy (2001), An episode of seafloor spreading and associated plate deformation inferred from crustal fluid pressure transients, *J. Geophys. Res.*, *106*(B10), 21,953–21,964, doi:10.1029/2000JB000040.

Davis, E. E., K. Becker, R. Dziak, J. Cassidy, K. Wang, and M. Lilley (2004), Hydrological response to a seafloor spreading regime on the Juan de Fuca ridge, *Nature*, *430*, 335–338.

Davis, E. E., A. LaBonte, J. He, K. Becker, and A. Fisher (2010), Thermally stimulated ‘‘runaway’’ downhole flow in a super-hydrostatic ocean-crustal borehole: Observations,

simulations, and inferences regarding crustal permeability, *J. Geophys. Res.*, *115*, B07102, doi:10.1029/2009JB006986.

Fisher, A. T. (1998), Permeability within basaltic oceanic crust, *Rev. Geophys.*, *36*(2), 143–182.

Fisher, A. T. (2005), Marine hydrogeology: Recent accomplishments and future opportunities, *Hydrogeol. J.*, *13*, 69–97, doi:10.1007/s10040-004-0400-y.

Fisher, A. T., K. Becker, and E. E. Davis (1997), The permeability of young oceanic crust east of Juan de Fuca ridge determined using borehole thermal measurements, *Geophys. Res. Lett.*, *24*(11), 1311–1314, doi:10.1029/97GL01286.

Fisher, A. T., et al. (2003a), Hydrothermal recharge and discharge across 50 km guided by seamounts on a young ridge flank, *Nature*, *421*, 618–621.

Fisher, A. T., et al. (2003b), Abrupt thermal transition reveals hydrothermal boundary and role of seamounts within the Cocos Plate, *Geophys. Res. Lett.*, *30*(11), 1550, doi:1510.1029/2002GL016766.

Fisher, A. T., T. Urabe, and A. Klaus, and the Expedition 301 Scientists (2005a), *Proceedings of the IODP*, vol. *301*, Integr. Ocean Drill. Program Manage. Int., College Station, Tex., doi:10.2204/iodp.proc.301.2005.

Fisher, A. T., et al. (2005b), Scientific and technical design and deployment of long-term, subseafloor observatories for hydrogeologic and related experiments, IODP Expedition 301, eastern flank of Juan de Fuca Ridge, *Proc. Integr. Ocean Drill. Program*, *301*, 1–39, doi:10.2204/iodp.proc.301.103.2005.

Fisher, A. T., E. E. Davis, and K. Becker (2008), Borehole-to-borehole hydrologic response across 2.4 km in the upper oceanic crust: Implications for crustal-scale properties, *J. Geophys. Res.*, *113*, B07106, doi:10.1029/2007JB005447.

Fisher, A. T., T. Tsuji, K. Petronotis, and the Expedition 327 Scientists (2011a), Proceedings of the IODP, vol. *327*, Integr. Ocean Drill. Program Manage. Int., Tokyo, doi:10.2204/iodp.proc.327.2011.

Fisher, A. T., et al. (2011b), Design, deployment, and status of borehole observatory systems used for single-hole and cross-hole experiments, IODP Expedition 327, eastern flank of the Juan de Fuca Ridge, *Proc. Integr. Ocean Drill. Program*, *327*, 1–38, doi:10.2204/iodp.proc.327.107.2011.

Fisher, A. T., J. Cowen, C. G. Wheat, and J. F. Clark (2011c), Preparation and injection of fluid tracers during IODP Expedition 327, eastern flank of Juan de Fuca Ridge, *Proc. Integr. Ocean Drill. Program*, *327*, 1–26, doi:10.2204/iodp.proc.327.108.2011.

Fisher, A. T., et al. (2012), Installing and servicing borehole crustal observatories to run three-dimensional cross-hole perturbation and monitoring experiments on the eastern flank of the Juan de Fuca Ridge: IODP Expedition 327 and Atlantis Expedition AT18-07, *Sci. Drill.*, *13*, 4–11, doi:10.2204/iodp.sd.13.01.2011.

Gavrilenko, P., and Y. Gueguen (1998), Flow in fractured media: A modified renormalization method, *Water Resour. Res.*, *34*(2), 177–191, doi:10.1029/97WR03042.

Graber, K. K., E. Pollard, G. Jonasson, and E. Schulte (Eds.) (2002), *Overview of Ocean Drilling Program engineering tools and hardware, ODP Tech. Note*, *31*, Ocean Drill. Program, College Station, Tex., doi:10.2973/odp.tn.31.2002.

Gregg, T. K. P., and D. J. Fornari (1998), Long submarine lava flows: Observations and results from numerical modeling, *J. Geophys. Res.*, *103*(B11), 27,517–27,531, doi:10.1029/98JB02465.

Hutnak, M., A. T. Fisher, L. Zühlsdorff, V. Spiess, P. Stauffer, and C. W. Gable (2006), Hydrothermal recharge and discharge guided by basement outcrops on 0.7–3.6 Ma seafloor east of the Juan de Fuca Ridge: Observations and numerical models, *Geochem. Geophys. Geosyst.*, *7*, Q07O02, doi:10.1029/2006GC001242.

Hutnak, M., A. T. Fisher, R. Harris, C. Stein, K. Wang, G. Spinelli, M. Schindler, H. Villinger, and E. Silver (2008), Large heat and fluid fluxes driven through mid-plate outcrops on ocean crust, *Nat. Geosci.*, *1*, 611–614, doi:10.1038/ngeo264.

Hyndman, R. D., R. P. Von Herzen, A. J. Erickson, and J. Jolivet (1976), Heat flow measurements in deep crustal holes on the Mid-Atlantic Ridge, *J. Geophys. Res.*, *81*(23), 4053–4060, doi:10.1029/JB081i023p04053.

Kappel, E. S., and W. B. F. Ryan (1986), Volcanic episodicity and a non-steady state rift valley along the northeast pacific spreading centers: Evidence from sea marc I, *J. Geophys. Res.*, *91*(B14), 13,925–13,940, doi:10.1029/JB091iB14p13925.

Karson, J. A. (2002), Geologic structure of the uppermost oceanic crust created at fast- to intermediate-rate spreading centers, *Annu. Rev. Earth Planet. Sci.*, *30*, 347–384.

Karson, J. A., M. A. Tivey, and J. R. Delaney (2002), Internal structure of uppermost oceanic crust along the Western Blanco Transform Scarp: Implications for subaxial accretion and deformation at the Juan de Fuca Ridge, *J. Geophys. Res.*, *107*(B9), 2181, doi:2110.1029/2000JB000051.

Khaleel, R. (1989), Scale dependence of continuum models for fractured basalts, *Water Resour. Res.*, *25*(8), 1847–1855, doi:10.1029/WR025i008p01847.

Macdonald, K. C., P. J. Fox, R. T. Alexander, and R. Pockalny (1996), Volcanic growth faults and the origin of Pacific abyssal hills, *Nature*, *380*, 125–129.

Matthews, M., M. Salisbury, and R. Hyndman (1984), *Basement logging on the Mid-Atlantic Ridge, Deep Sea Drilling Project Hole 395A, in Initial Reports, DSDP*, edited by R. D. Hyndman and M. H. Salisbury, pp. 717–730, U.S. Gov. Print. Off., Washington, D. C.

Nedimovic, M. R., S. M. Carbotte, J. P. Canales, J. B. Diebold, A. J. Harding, and G. M. Kent (2008), Upper crustal evolution along the Juan de Fuca Ridge flanks, *Geochem. Geophys. Geosyst.*, *9*, Q09006, doi:10.1029/2008GC002085.

Neuman, S. P. (2005), Trends, prospects and challenges in quantifying flow and transport through fractured rocks, *Hydrogeol. J.*, *13*, 124–147, doi:10.1007/s10040-004-0397-2.

Pezard, P., and R. N. Anderson (1989), Morphology and alteration of the upper oceanic crust from in-situ electrical experiments in DSDP/ODP Hole 504B, *Proc. Integr. Ocean Drill. Program Sci. Results*, *111*, 133–146.

Pezard, P. A., R. N. Anderson, W. B. F. Ryan, K. Becker, J. C. Alt, and P. Gente (1992), Accretion, structure, and hydrology of intermediate spreading-rate oceanic crust from drill-hole experiments and seafloor observations, *Mar. Geophys. Res.*, *14*, 93–123.

Rovey, C. W., and D.S Cherkauer (1995), Scale dependency of hydraulic conductivity measurements, *Ground Water*, *33*, 769–780.

Schmincke, H.-U., and U. Bednarz (1990), *Pillow, sheet flow, and breccia flow volcanoes and volcano-tectonic-hydrothermal cycles in the extrusive series of the northeastern Troodos ophiolite, Cyprus, in Proceedings of the Symposium ''Troodos '87'' on Ophiolites: Ocean Crustal Analogues*, edited by J. Malpas et al., pp. 185–206, Geol. Surv. Dep., Nicosia.

Shipboard Scientific Party (2011), *Site U1362, in Proceedings of the Ocean Drilling Program, Initial Reports*, edited by A. T. Fisher, T. Tsuji, and K. Petronotis, Integr. Ocean Drill. Program, College Station, Tex., *301*, 1–97, doi:10.2204/iodp.proc.327.103.2011.

Theis, C. V. (1935), The lowering of the piezometer surface and the rate and discharge of a well using ground-water storage, *Eos Trans. AGU*, *16*, 519–524.

Wheat, C. G., and A. T. Fisher (2008), Massive, low-temperature hydrothermal flow from a basaltic outcrop on 23 Ma seafloor of the Cocos Plate: Chemical constraints and implications, *Geochem. Geophys. Geosyst.*, *9*, Q12O14, doi:10.1029/2008GC002136.

Wheat, C. G., H. Elderfield, M. J. Mottl, and C. Monnin (2000), Chemical composition of basement fluids within an oceanic ridge flank: Implications for along-strike and across-strike hydrothermal circulation, *J. Geophys. Res.*, *105*(B6), 13,437–13,447, doi:10.1029/2000JB900070.

Zhou, H., L. Li, and J. J. Gómez-Hernández (2010), Three-dimensional hydraulic conductivity upscaling in groundwater modeling, *Comput. Geosci.*, *36*, 1224–1235.

Zhu, W., D. K. Smith, and L. G. J. Montési (2003), Effects of regional slope on viscous flows: A preliminary study of lava terrace emplacement at submarine volcanic rift zones, *J. Volcanol. Geotherm. Res.*, *119*(1–4), 145–159.

Zühlsdorff, L., M. Hutnak, A. T. Fisher, V. Spiess, E. E. Davis, M. Nedimovic, S. Carbotte, H. Villinger, and K. Becker (2005), Site surveys related to IODP Expedition 301: Image-Flux (SO149) and RetroFlux (TN116) expeditions and earlier studies, *Proc. Integr. Ocean Drill. Program*, *301*, 1–48, doi:10.2204/iodp-proc.301.102.2005.